A role for PKC-ε in FcγR-mediated phagocytosis by RAW 264.7 cells

Elaine C. Larsen,[1] Takehiko Ueyama,[3] Pamela M. Brannock,[1] Yasuhito Shirai,[3] Naoaki Saito,[3] Christer Larsson,[4] Daniel Loegering,[2] Peter B. Weber,[5] and Michelle R. Lennartz[1]

Centers for [1]Cell Biology and Cancer Research and [2]Cardiovascular Sciences, Albany Medical College, Albany, NY 12208
[3]Laboratory of Molecular Pharmacology, Biosignal Research Center, Kobe University, 1-1 Rokkodai-cho, Nada-ku, Kobe 657-8501, Japan
[4]Department of Laboratory Medicine, Molecular Medicine, Malmo University Hospital, S-205 02 Malmo, Sweden
[5]Waste Reduction by Waste Reduction, Inc., 1 University Place, Rensselaer, NY 12144

Protein kinase C (PKC) plays a prominent role in immune signaling, and the paradigms for isoform selective signaling are beginning to be elucidated. Real-time microscopy was combined with molecular and biochemical approaches to demonstrate a role for PKC-ε in Fcγ receptor (FcγR)–dependent phagocytosis. RAW 264.7 macrophages were transfected with GFP-conjugated PKC isoforms, and GFP movement was followed during phagocytosis of fluorescent IgG–opsonized beads. PKC-ε, but not PKC-δ, concentrated around the beads. PKC-ε accumulation was transient; apparent as a "flash" on target ingestion. Similarly, endogenous PKC-ε was specifically recruited to the nascent phagosomes in a time-dependent manner. Overexpression of PKC-ε, but not PKC-α, PKC-δ, or PKC-γ enhanced bead uptake 1.8-fold. Additionally, the rate of phagocytosis in GFP PKC-ε expressors was twice that of cells expressing GFP PKC-δ. Expression of the regulatory domain (εRD) and the first variable region (εV1) of PKC-ε inhibited uptake, whereas the corresponding PKC-δ region had no effect. Actin polymerization was enhanced on expression of GFP PKC-ε and εRD, but decreased in cells expressing εV1, suggesting that the εRD and εV1 inhibition of phagocytosis is not due to effects on actin polymerization. These results demonstrate a role for PKC-ε in FcγR-mediated phagocytosis that is independent of its effects on actin assembly.

Introduction

Ligation of macrophage Fcγ receptors (FcγR)* elicits phagocytosis, pathogen killing, and gene activation. The involvement of PKC in these processes is well documented, although less is known about which PKC isoforms transduce the relevant signals (Foreback et al., 1998; Korchak et al., 1998; Karimi et al., 1999; Melendez et al., 1999; Dekker et al., 2000; Kontny et al., 2000).

The PKC isoforms are divided into three families: (1) cPKC-α, -βI, -βII, and -γ require Ca^{2+}, DAG, and phosphatidylserine (PS); (2) nPKC-ε, -δ, -θ, and -η require DAG and PS; and (3) aPKC-ζ and -ι/λ require PS (Nishikawa et al., 1997). All PKCs contain a unique regulatory and a homologous catalytic domain, but have little substrate specificity in vitro (Nishikawa et al., 1997). In cells, isoform-selective PKC translocation occurs in response to stimuli, suggesting that the regulatory domain contains critical targeting information (Yedovitzky et al., 1997). Indeed, isoform-specific docking proteins have been identified that bind to the C2 region of the regulatory domain (Ron et al., 1994; Prekeris et al., 1996; Csukai et al., 1997). Additionally, the regulatory domain C1 region binds membrane lipids, including DAG, arachidonic acid, and ceramide (Kashiwagi et al., 2002). These results suggest that PKCs have multiple mechanisms for membrane localization, but how these regions direct PKCs to their site of action and lead to their activation is not well understood. GFP-conjugated PKC isoforms have been used extensively to probe signaling pathways in mammalian cells. These chimeras have enzymatic and activation properties similar to their endogenous counterparts and provide convenient readouts for PKC movement on cell stimulation (Sakai et al., 1997; Ohmori et al., 1998; Shirai et al., 1998; Wang et al., 1999).

The online version of this article contains supplemental material.

*Abbreviations used in this paper: FcγR, Fcγ receptor; BIgG, IgG-opsonized glass beads; EIgG, IgG-opsonized erythrocytes; εRD, regulatory domain of PKC-ε; δV1, first region fragment of PKC-δ; εV1, first variable region of PKC-ε.

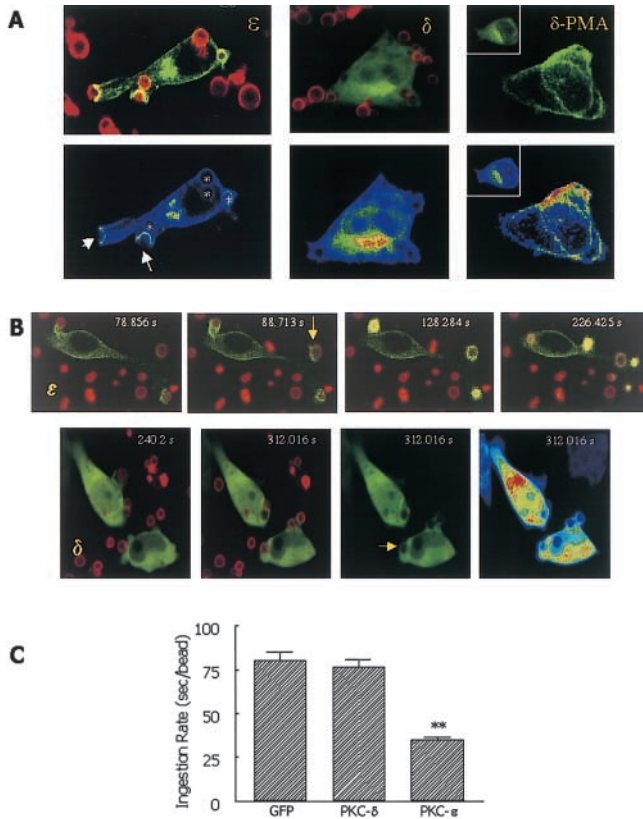Key words: protein kinase C-epsilon; macrophage; confocal; signal transduction; immunoglobulin

Figure 1. **PKC-ε, but not PKC-δ, localizes to targets during IgG-mediated phagocytosis.** (A) Transfectants expressing GFP-conjugated PKC-ε or PKC-δ were incubated with Alexa 568 BIgG for 10 min, fixed, and analyzed by confocal microscopy. A Z series was taken and a single image was presented. (A) Top, merge of green and red. Bottom, pseudocolor highlighting the relative concentration of the GFP (cool colors = low concentrations, warm colors = higher concentrations). Left, Phagocytic cups (arrows) and newly formed phagosomes (+) have accumulated PKC-ε, internalized particles have background levels (asterisk; $n > 10$). Middle, GFP PKC-δ does not concentrate around targets. Right, PMA (10 μM, 8 min) stimulates nuclear and plasma membrane localization of GFP PKC-δ. Inset, same cell before PMA. (B) Cells were transfected with GFP PKC-ε (ε) or GFP PKC-δ (δ). Images were taken at 10-s intervals after addition of BIgG (Videos 1 and 2). PKC-ε panel 1, binding; panel 2, first accumulation; panel 3, ingestion complete; panel 4, loss of concentration. PKC-δ panel 1, binding; panel 2, ingestion complete. Time for ingestion: PKC-ε, 49.43 s; PKC-δ, 71.82 s. Total time that PKC-ε is concentrated: 137.71 s. Evaluating the green signal alone facilitates determination of ingestion (PKC-δ panel 3, first frame in which bead is completely surrounded by green). PKC-δ panel 4: pseudocolor demonstrating that PKC-δ does not accumulate at targets ($n > 20$). (C) Quantitation of ingestion rate. Time was calculated from first indentation of membrane to first frame in which target was surrounded by GFP. PKC-δ, $n = 49$; PKC-ε, $n = 35$; GFP, $n = 69$ from 4–7 experiments. **, $P < .001$. Videos 1 and 2 are available at http://www.jcb.org/cgi/content/full/jcb.200205140/DC1.

During IgG-dependent phagocytosis, molecules that translocate to the phagosome are implicated in subsequent signaling events. We have demonstrated that PKC-α, PKC-δ, and PKC-ε translocate to membranes during phagocytosis, and PKC-α and PKC-ε are present in phagosomes (Allen and Aderem, 1995; Brumell et al., 1999; Larsen et al., 2000). That PKC inhibitors block phagocytosis in monocytes and macro-

phage cell lines verifies their involvement in the ingestion process (Zheleznyak and Brown, 1992; Karimi and Lennartz, 1998; Karimi et al., 1999; Larsen et al., 2000). Recently, we reported that a cPKC is necessary for FcγR-stimulated respiratory burst, but that an nPKC is involved in phagocytosis (Larsen et al., 2000). The present study identifies a role for nPKC-ε in FcγR-mediated phagocytosis.

Results and discussion
PKC-ε localizes to IgG-containing phagosomes
RAW 264.7 macrophages (RAW cells) express nPKCs-δ and -ε (Larsen et al., 2000). Because it is involved in other actin-based processes, we tested the hypothesis that PKC-ε is necessary for IgG-mediated phagocytosis (Zeidman et al., 1999; Berrier et al., 2000). Initially, GFP-conjugated PKC-ε and -δ were visualized in fixed cells after synchronized phagocytosis of Alexa 568–labeled IgG-opsonized glass beads (BIgG). Three patterns were seen that predominated at different ingestion times (Fig. 1 A, ε; depicted in a single cell at 10 min of phagocytosis). Initially, PKC-ε accumulated at phagocytic cups (arrows); by 5 min, internalized beads with high PKC-ε levels were detected (+). At 10 min, many targets had lost the GFP concentration (asterisk). In contrast, the distribution of GFP PKC-δ was not altered (Fig. 1 A, δ). These results suggest that PKC-ε transiently associates with targets, accumulating on particle binding and dissociating after phagosome closure.

The localization of GFP PKC-ε in fixed cells was confirmed by real-time imaging. PKC-ε accumulation was seen as a "flash" as targets were ingested (Fig. 1 B, ε; Video 1, available at http://www.jcb.org/cgi/content/full/jcb.200205140/DC1). A localization time of 131 ± 11 s ($n = 26$, 4 experiments) was calculated from the first concentration of GFP until the signal returned to cytosolic levels. GFP concentration preceded phagosome closure and dispersed after ingestion. These observations are consistent with a role for PKC-ε in phagocytosis. No change in PKC-δ distribution was detected (Fig.1 B, δ; Video 2, available at http://www.jcb.org/cgi/content/full/jcb.200205140/DC1), although its translocation in re-
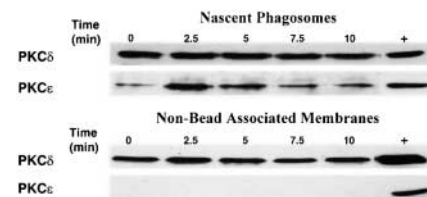

Figure 2. **Localization of endogenous PKC-ε and PKC-δ during IgG-mediated phagocytosis.** Synchronized phagocytosis was performed as described in Materials and methods. At varying times (0–10 min), phagocytosis was terminated, and nascent phagosomes and nonbead-associated membranes were recovered and subjected to immunoblot analysis for PKC-ε. The same membrane was then reprobed for PKC-δ. PKC-ε translocates to nascent phagosomes in a time-dependent fashion. PKC-δ is present in both phagosomes and membranes, and levels do not change. Data are representative of four experiments. Rat brain lysate was used as a positive control for the antibodies (+ lane).

sponse to PMA confirmed that the construct was functional (Fig. 1 A, δ-PMA).

To follow translocation of endogenous PKCs, we isolated nascent phagosomes from untransfected cells at varying times during synchronized phagocytosis. PKC-ε levels were elevated in 2.5–7.5-min phagosomes, but not in the non-bead-associated membranes (Fig. 2). In contrast, PKC-δ was present in both phagosomes and membranes; a small (but reproducible) increase was seen in membranes at 2.5 min, but the level in phagosomes did not change (Fig. 2). These results demonstrate that GFP-conjugated PKCs mimic their endogenous isoforms with respect to FcγR-dependent translocation, and can be used as reporters for them.

Previously, we reported that PKC-δ and PKC-ε translocate to (unfractionated) membranes during phagocytosis (Larsen et al., 2000). Figs. 1 and 2 reveal that the increase in membrane levels occurs at the phagosome for PKC-ε and at the nonbead-associated membranes for PKC-δ. Thus, PKC-δ may be involved in nonphagocytic FcγR signaling processes, e.g., gene regulation. Indeed, that PMA stimulated nuclear translocation of GFP PKC-δ in our cells (Fig. 1 A, δ-PMA) is consistent with this hypothesis and published reports (Wang et al., 1999).

Modulation of PKC-ε alters IgG-mediated phagocytosis

To determine if PKC-ε is involved in FcγR-mediated phagocytosis, we quantified BIgG uptake in cells expressing full-length GFP PKC-α, PKC-δ, PKC-ε, or PKC-γ. Controls received unconjugated GFP. Immunoblot analysis revealed that PKC-α, PKC-δ, and PKC-γ were expressed at levels 10-fold higher than the endogenous enzyme; PKC-ε expression increased fourfold (unpublished data). Only expression of GFP PKC-ε increased ingestion. The enhancement was 1.8-fold (Fig. 3, $P < .001$), similar to that obtained on PMA/DAG treatment (Larsen et al., 2000). That overexpression of PKC-ε increased phagocytosis supports a
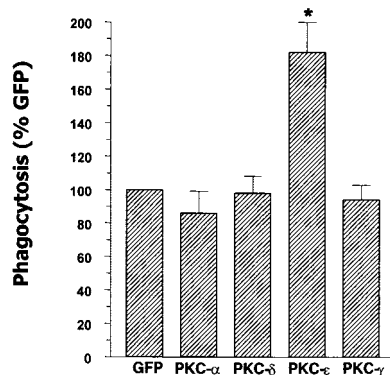
role for this isoform in phagocytosis. The fact that no other isoform affected ingestion indicates that PKC overexpression, per se, does not modulate FcγR signaling.

The rate of phagocytosis was determined by subtracting the time of the first indentation of the membrane from that at which the particle was encircled with GFP. Phagocytosis in PKC-δ and GFP overexpressors was 76 ± 4 s/bead and 80 ± 5 s/bead, respectively, but 35 ± 2 s/bead for PKC-ε (Fig. 1 C). Thus, beads were taken up twice as fast in the PKC-ε versus the GFP or PKC-δ overexpressors ($P < .001$), resulting in the enhancement seen in Fig. 3.

Inhibitory fragments of PKC-ε depress phagocytosis

The first variable region of PKC-δ and PKC-ε (δV1 and εV1) associates with PKC docking proteins on membranes, preventing binding of the full length enzyme and acting as isoform-specific inhibitors (Hundle et al., 1997; Yedovitzky et al., 1997; Mochly-Rosen and Gordon, 1998; Zeidman et al., 1999). We determined the effect of expression of GFP-δV1 and εV1 on phagocytosis in RAW cells. Although expressed at equivalent levels (unpublished data), phagocytosis was decreased 50% in cells expressing εV1 compared with GFP controls; uptake in δV1 expressors was not different from GFP alone (Fig. 4).

We also tested the regulatory domain fragment of PKC-ε (εRD) for its effects on phagocytosis. This domain is necessary and sufficient for neurite extension (Zeidman et al., 1999). If neurite and pseudopod extension are similar, εRD should support phagocytosis. Alternatively, if catalytic activity is necessary, εRD should block localization of the intact PKC-ε and inhibit phagocytosis. Transfectants expressing εRD had significantly lower phagocytosis than those expressing unconjugated GFP or GFP δV1 (Fig. 4). Additionally, εRD localized to phagocytic cups (Fig. 4 B). These findings suggest that the catalytic activity of PKC-ε is necessary for phagocytosis.

To determine if the inhibitory effects of εRD and εV1 were due to defects in actin assembly, we quantified phalloi-

Figure 3. **Overexpression of PKC-ε alters phagocytosis.** RAW cells were transfected with GFP-conjugated PKC-α, PKC-δ, PKC-ε, or PKC-γ. Unconjugated GFP was used as the control. Cells were incubated for 60 min with dextran-rhodamine–loaded EIgG, and phagocytosis was quantified in >100 transfected cells. Results are reported as the percentage of phagocytosis measured in cells expressing unconjugated GFP ($n = 3$; *, $P < .01$). Transfection alone did not alter phagocytosis, as uptake in GFP controls was equivalent to that in untransfected cells (not depicted).
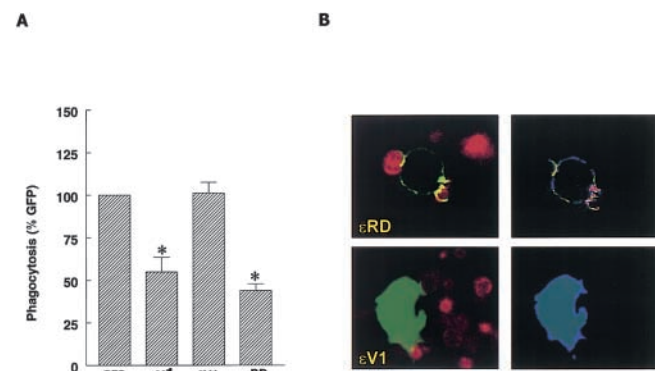

Figure 4. **Expression of GFP-conjugated fragments depresses phagocytosis.** Cells were transfected with plasmids encoding the V1 region of PKC-ε (εV1) or PKC-δ (δV1), or the regulatory domain of PKC-ε (εRD). (A) Phagocytosis was performed as in Figure 3. (B) Confocal analysis of εRD and εV1 demonstrates that εRD concentrates at targets. Concentration of εV1 was not observed, possibly due to a rapid cycling to and from the membrane ($n = 3$–9). *, $P < .01$.
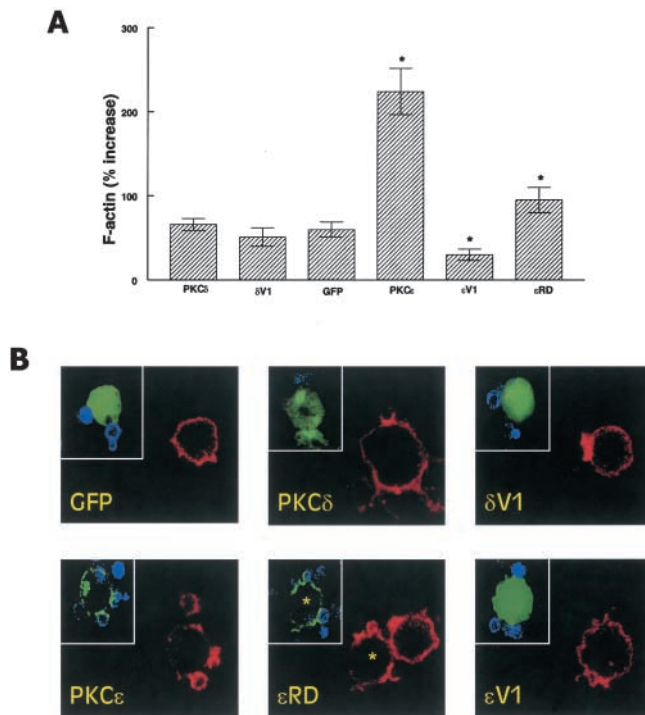
Figure 5. **Expression of PKC-ε constructs alters actin assembly.** Cells were transfected with PKC-δ, δ V1, GFP (control), PKC-ε, εV1, or εRD and were subjected to synchronized phagocytosis for 2 min, fixed, and the actin was visualized with Alexa 660–phalloidin. (A) Actin accumulation in PKC-ε ($n = 32$) and εRD ($n = 33$) cells was significantly higher than GFP controls ($n = 33$). Expression of εV1 ($n = 24$) decreased actin assembly. PKC-δ ($n = 29$) and δV1 ($n = 25$) levels were similar to GFP ($n = 33$). *, $P < 0.05$. (B) Visualization of PKC (green), actin (red), or targets (blue) in representative cells.

din fluorescence at the phagocytic cup (Fig. 5). The accumulation of actin was similar for GFP controls and cells expressing PKC-δ and δV1. A substantial increase in actin was detected in cells expressing GFP PKC-ε. However, despite similar effects on phagocytosis, the actin accumulation in εV1 expressors was significantly lower ($P < 0.02$), and that in εRD was significantly higher ($P < 0.04$) than that in the GFP-expressing controls. The fact that PKC-ε and εRD contain an actin-binding domain (Prekeris et al., 1996) is consistent with their ability to accumulate actin. In contrast, εV1 may block localization of endogenous PKC-ε, interfering with normal actin polymerization and resulting in decreased actin assembly. Together, these data suggest that the inhibitory effect of εRD and εV1 is not due to effects on actin assembly. Rather, the results support the hypothesis that the PKC-ε regulatory domain localizes the catalytic domain to phagosomes where it phosphorylates critical components of the phagocytic machinery. This is consistent with reports that PKC inhibitors block phagocytosis (Zheleznyak and Brown, 1992; Larsen et al., 2000).

PKC-ε and εRD localized only to the forming phagosome, suggesting that specific interaction(s) that direct them there. The εV1 fragment associates with phagocytic complexes and inhibits phagocytosis, suggesting the regulation of PKC-ε translocation is dependent on the V1 region. PKC-ε may be recruited to the site of FcγR ligation by se-

lective protein–protein interactions. β-COP is a binding protein for PKC-ε (Csukai et al., 1997) and is necessary for phagocytosis (Hackam et al., 2001). Thus, it may function to direct PKC-ε to the phagosome for propagation of the phagocytic signal.

Because manipulation of PKC-ε levels correlated with partial inhibition of phagocytosis, it may not be the only isoform involved. RAW cells expressing dominant negative PKC-α have impaired phagocytosis (Breton and Descoteaux, 2000). However, in our cells PKC-α enters the phagosome ∼10 min after initiation of phagocytosis (unpublished data). By this time, PKC-ε levels are decreasing (Fig. 2), so it is possible that PKC-ε mediates initial phagocytosis and PKC-α supports ingestion at later times.

Materials and methods

Materials
EDTA, EGTA, BSA, thimersol, ammonium persulfate, Triton X-100, sucrose, DTT, DMSO, and NaOH were obtained from Sigma-Aldrich. Tris base, SDS, $CaCl_2$ and $MgCl_2$ were purchased from Mallinckrodt Baker, Inc. Construction of the GFP PKC plasmids has been described previously (Ohmori et al., 1998; Shirai et al., 1998; Zeidman et al., 1999).

Buffers
$HBSS^{2+}$ consists of the following: HBSS (Life Technologies) containing 4 mM sodium bicarbonate, 10 mM Hepes, and 1.5 mM $CaCl_2$ and $MgCl_2$. Lysis buffer consists of 25 mM Tris-HCl, pH 7.4, 0.25 M sucrose, 2.5 mM DTT, and 2.5 mM EDTA (5 mM benzamidine, 50 μg/ml leupeptin, 50 μg/ml aprotinin, 50 μg/ml trypsin inhibitor, 5 μg/ml pepstatin, 1 mM phenylmethylsulfonyl fluoride, 20 mM NaF, 1 mM Na_3VO_4, 1 mM paranitrophenyl phosphate, and 5 mM imidazole; Sigma-Aldrich). DNA assay buffer consists of 2 M NaCl, 2 mM EDTA and 50 mM Na_2HPO_4. TBST consists of 50 mM Tris, pH 7.5, 150 mM NaCl, 0.05% Tween 20 and 0.01% thimersol.

Cells
The RAW LacR/FMLPR.2 subclone of RAW 264.7 cells was received from Dr. Steven Greenberg (Columbia University, New York, NY; Cox et al., 1997). Cells were maintained in RPMI 1640 (GIBCO BRL), sodium pyruvate, nonessential amino acids, glutamate (BioWhittaker), and 10% newborn calf serum (HyClone).

Transfections
Phagocytosis assays and confocal analysis on fixed cells were described previously (Larsen et al., 2000). For real-time confocal experiments, 10^6 cells were plated onto 35-mm glass bottom plates (MatTek Corporation) and transfected using 1 μg of DNA (Larsen et al., 2000). Cells were imaged 24–30 h after transfection.

Targets
Phagocytosis in transfected cells was quantified using IgG-opsonized erythrocytes (EIgG) loaded with dextran-rhodamine (Scott et al., 1990); BIgG for nascent phagosome isolation were made as described previously (Karimi and Lennartz, 1995). 5 μg Alexa 568–conjugated BSA (Molecular Probes, Inc.) was included in the BSA coating step for generation of fluorescent BIgG.

Synthesis of dextran-rhodamine
2.4 g 10K dextran was dissolved in 20 ml DMSO in a Teflon-lined screw-cap tube. 233 mg of rhodamine B isothiocyanate, 0.5 ml of ferric chloride in 183 mg/ml acetylacetone, and 0.5 ml of ferric chloride in 210 mg/ml pyridine was added, and the mixture was heated at 120°C for 3 h. After cooling, the solution was poured into 400 ml of 95% ethanol containing 10 g of sodium acetate. The dextran–rhodamine conjugate settled out for 3 h and was reprecipitated in 400 ml of 95% ethanol (at 10°C for 16 h), filtered, and suction-dried. The product was dissolved in 30 ml of water and loaded onto a 4 × 50-cm fine column (Sephadex G25; Amersham Biosciences). 20-ml fractions were collected and analyzed for their spectra. Fractions 12–17 were pooled, lyophilized, and analyzed for dye content (by absorbance at 543 nm) and hexose content (phenol sulfuric acid method; Dubois et al., 1956). 9.37 nmol rhodamine ± 4.4% per mg dextran was calculated.

Phagocytosis assays

Dextran-rhodamine–loaded EIgG were added to transfectants at a 10:1 ratio. After 60 min, extracellular targets were lysed and the coverslips were mounted using ProLong® Antifade (Molecular Probes, Inc.). Targets were counted in >100 transfected cells, and the phagocytic index was calculated (Larsen et al., 2000). The results are normalized to cells expressing unconjugated GFP. All measurements were made in triplicate on three or more separate cell preparations. Data are expressed as the mean ± SEM. Comparisons were made by ANOVA.

For confocal analysis, BIgG (4/cell) were bound to transfected cells (15 min on ice). The cells were placed in a 37°C water bath and fixed at 2.5–10 min. The coverslips were mounted onto slides and imaged as described previously (Larsen et al., 2000).

Nascent phagosomes

Cells were plated in 10-cm dishes and used when 90% confluent (∼12 × 10^6 cells/plate). Cells were washed with HBSS and chilled on ice. BIgG (30/cell) were bound (15 min) and then warmed to 37°C for synchronized phagocytosis. At the indicated times, cells were scraped into lysis buffer and sonicated (2 × 20 s, 2-s pulses). The beads were allowed to settle 1 h on ice. The supernatant was removed and the beads were washed once with lysis buffer and then solubilized in SDS sample buffer. Nonbead-associated membranes were recovered from the supernatant by ultracentrifugation. The resulting pellet was extracted with lysis buffer + 1% Triton X-100. SDS-PAGE was run on the nascent phagosomes (normalized for number of beads) and nonbead-associated membranes (normalized for DNA; Labarca and Paigen, 1980). After SDS-PAGE, the proteins were transferred to nitrocellulose for immunoblot analysis (Larsen et al., 2000). Primary antibody (monoclonal, PKC-α and PKC-δ; Transduction Laboratories; polyclonal, anti-PKC-ε; Santa Cruz Biotechnology, Inc.) was followed by secondary antibody (goat anti–rabbit HRP; Santa Cruz Biotechnology, Inc.) or rabbit anti–mouse HRP (Jackson ImmunoResearch Laboratories). Bands were detected with SuperSignal ECL (Pierce Chemical Co.).

Phalloidin staining

Transfected cells were fixed after 2 min of synchronized phagocytosis (Larsen et al., 2000), permeabilized (30 min, 0.1% Triton X-100 in 1% BSA in PBS), and stained with 0.7 µM Alexa 660–conjugated phalloidin (for 60 min at 22°C). Coverslips were washed in PBS, mounted, and imaged (Larsen et al., 2000). Pixel density at the phagocytic cup was quantified using the Intervision 2D analysis program (Noran Instruments, Inc.), and was normalized to the pixel density of an equivalent area of nontarget-associated membrane. Normalized data for 24–33 events/condition from four independent experiments were compared with GFP controls using the t test.

Online supplemental material

Phagocytosis of IgG-coated glass beads was followed with time using an inverted confocal laser scanning fluorescence microscope (LSM 410; Carl Zeiss MicroImaging, Inc.) with a heated stage and 40× oil objective. GFP was visualized using 488-nm argon excitation and a 505–550 barrier filter; Alexa 568 was detected using 543-nm HeNe excitation and a 560 long pass barrier filter. For each experiment, the media was removed and replaced with 800 µl HBSS^{2+}. 200 µl HBSS^{2+} containing 2 × 10^6 BIgG was added to each plate (4:1 target; macrophage). Cells expressing GFP-conjugated PKCs were located and BIgG were added. Data collection began when the beads first contacted the cells. The GFP and Alexa images were collected simultaneously at 10-s intervals for 10 min. Videos 1 and 2 represent more than 20 independent experiments with each isoform. Online supplemental material available at http://www.jcb.org/cgi/content/full/jcb.200205140/DC1.

References

Allen, L.-A.H., and A. Aderem. 1995. A role for MARCKS, the PKC-α, and myosin I in zymosan phagocytosis by macrophages. *J. Exp. Med.* 182:829–840.

Berrier, A.L., A.M. Mastrangelo, J. Downward, M. Ginsberg, and S.E. LaFlamme. 2000. Activated R-ras, Rac1, PI 3-kinase and PKC-ε can each restore cell spreading inhibited by isolated integrin β1 cytoplasmic domains. *J. Cell Biol.* 151:1549–1560.

Breton, A., and A. Descoteaux. 2000. PKC-α participates in FcγR-mediated phagocytosis in macrophages. *Biochem. Biophys. Res. Commun.* 276:472–476.

Brumell, J.H., J.C. Howard, K. Craig, S. Grinstein, A.D. Schreiber, and M. Tyers. 1999. Expression of the PKC substrate pleckstrin in macrophages: association with phagosomal membranes. *J. Immunol.* 163:3388–3395.

Cox, D., P. Chang, Q. Zhang, P.G. Reddy, G.M. Bokoch, and S. Greenberg. 1997. Requirements for both Rac1 and Cdc42 in membrane ruffling and phagocytosis in leukocytes. *J. Exp. Med.* 186:1487–1494.

Csukai, M., C.H. Chen, M.A. De Matteis, and D. Mochly-Rosen. 1997. The coatomer protein β′-COP, a selective binding protein (RACK) for PKC-ε. *J. Biol. Chem.* 272:29200–29206.

Dekker, L.V., M. Leitges, G. Altschuler, N. Mistry, A. McDermott, J. Roes, and A.W. Segal. 2000. PKC-β contributes to NADPH oxidase activation in neutrophils. *Biochem. J.* 347:285–289.

Dubois, M., K.A. Gilles, J.K. Hamilton, P.A. Rebers, and F. Smith. 1956. Colorimetric method for the determination of sugars and related substances. *Anal. Chem.* 28:350–356.

Foreback, J.L., V. Sarma, N.R. Yeager, E.M. Younkin, D.G. Remick, and P.A. Ward. 1998. Blood mononuclear cell production of TNF-α and IL-8: engagement of different signal transduction pathways including the p42 MAP kinase pathway. *J. Leukoc. Biol.* 64:124–133.

Hackam, D.J., R.J. Botelho, C. Sjolin, O.D. Rotstein, J.M. Robinson, A.D. Schreiber, and S. Grinstein. 2001. Indirect role for COPI in the completion of FCγ receptor-mediated phagocytosis. *J. Biol. Chem.* 276:18200–18208.

Hundle, B., T. McMahon, J. Dadgar, C.H. Chen, D. Mochly-Rosen, and R.O. Messing. 1997. An inhibitory fragment derived from PKC-ε prevents enhancement of nerve growth factor responses by ethanol and phorbol esters. *J. Biol. Chem.* 272:15028–15035.

Karimi, K., T.R. Gemmill, and M.R. Lennartz. 1999. PKC and a calcium-independent phospholipase are required for IgG-mediated phagocytosis by Mono-Mac-6 cells. *J. Leukoc. Biol.* 65:854–862.

Karimi, K., and M.R. Lennartz. 1995. PKC activation precedes arachidonic acid release during IgG-mediated phagocytosis. *J. Immunol.* 155:5786–5794.

Karimi, K., and M.R. Lennartz. 1998. MAP kinase is activated during IgG-mediated phagocytosis but is not required for target ingestion. *Inflammation.* 22:67–82.

Kashiwagi, K., Y. Shirai, M. Kuriyama, N. Sakai, and N. Saito. 2002. Importance of C1B domain for lipid messenger-induced targeting of PKC. *J. Biol. Chem.* 277:18037–18045.

Kontny, E., M. Kurowska, K. Szczepanska, and W. Maslinski. 2000. Rottlerin, a PKC isozyme-selective inhibitor, affects signaling events and cytokine production in human monocytes. *J. Leukoc. Biol.* 67:249–258.

Korchak, H.M., M.W. Rossi, and L.E. Kilpatrick. 1998. Selective role for β-PKC in signaling for O-2 generation but not degranulation or adherence in differentiated HL60 cells. *J. Biol. Chem.* 273:27292–27299.

Labarca, C., and K. Paigen. 1980. A simple, rapid, and sensitive DNA assay procedure. *Anal. Biochem.* 102:344–352.

Larsen, E.C., J.A. DiGennaro, N. Saito, S. Matha, D.J. Loegering, J.M. Mazurkiewicz, and M.R. Lennartz. 2000. Differential requirement for classic and novel PKC isoforms in respiratory burst and phagocytosis in RAW 264.7 cells. *J. Immunol.* 165:2809–2817.

Melendez, A.J., M.M. Harnett, and J.M. Allen. 1999. Differentiation-dependent switch in PKC isoenzyme activation by FcγRI, the human high-affinity receptor for immunoglobulin G. *Immunology.* 96:457–464.

Mochly-Rosen, D., and A.S. Gordon. 1998. Anchoring proteins for PKC: a means for isozyme selectivity. *FASEB J.* 12:35–42.

Nishikawa, K., A. Toker, F.J. Johannes, Z. Songyang, and L.C. Cantley. 1997. Determination of the specific substrate sequence motifs of PKC isozymes. *J. Biol. Chem.* 272:952–960.

Ohmori, S., Y. Shirai, N. Sakai, M. Fujii, H. Konishi, U. Kikkawa, and N. Saito. 1998. Three distinct mechanisms for translocation and activation of the delta subspecies of PKC. *Mol. Cell. Biol.* 18:5263–5271.

Prekeris, R., M.W. Mayhew, J.B. Cooper, and D.M. Terrian. 1996. Identification and localization of an actin-binding motif that is unique to PKC-ε and participates in the regulation of synaptic function. *J. Cell Biol.* 132:77–90.

Ron, D., C.-H. Chen, J. Caldwell, L. Jamieson, E. Orr, and D. Mochly-Rosen. 1994. Cloning of an intracellular receptor for PKC: A homolog of the β subunit of G proteins. *Proc. Natl. Acad. Sci. USA.* 91:839–843.

Sakai, N., K. Sasaki, N. Ikegaki, Y. Shirai, Y. Ono, and N. Saito. 1997. Direct visualization of the translocation of the γ-subspecies of protein kinase C in living cells using fusion proteins with green fluorescent protein. *J. Cell Biol.* 139: 1465–1476.

Scott, M.D., F.A. Kuypers, P. Butikofer, R.M. Bookchin, O. Ortix, and B.H. Lubin. 1990. Effect of osmotic lysis-resealing on resealing on red cell structure and function. *J. Lab. Clin. Med.* 115:470–480.

Shirai, Y., K. Kashiwagi, K. Yagi, N. Sakai, and N. Saito. 1998. Distinct effects of fatty acids on translocation of γ- and ε- subspecies of PKC. *J. Cell Biol.* 143: 511–521.

Wang, Q.J., D. Bhattacharyya, S. Garfield, K. Nacro, V.E. Marquez, and P.M. Blumberg. 1999. Differential localization of PKC-δ by phorbol esters and related compounds using a fusion protein with green fluorescent protein. *J. Biol. Chem.* 274:37233–37239.

Yedovitzky, M., D. Mochly-Rosen, J.A. Johnson, M.O. Gray, D. Ron, E. Abramovitch, E. Cerasi, and R. Nesher. 1997. Translocation inhibitors define specificity of PKC isoenzymes in pancreatic β-cells. *J. Biol. Chem.* 272:1417–1420.

Zeidman, R., B. Lofgren, S. Pahlman, and C. Larsson. 1999. PKC-ε, via its regulatory domain and independently of its catalytic domain, induces neurite-like processes in neuroblastoma cells. *J. Cell Biol.* 145:713–726.

Zheleznyak, A., and E.J. Brown. 1992. Immunoglobulin-mediated phagocytosis by human monocytes requires PKC activation. *J. Biol. Chem.* 267:12042–12048.